FACILE SYNTHESIS OF Ag-AgCl/ZnO HYBRID WITH HIGH EFFICIENCY PHOTOCATALYTIC PROPERTY UNDER VISIBLE LIGHT

L. FU[a], Y. ZHENG[a*], Z. WANG[a], A. WANG[b], L. HE[d], B. DENG[c], F. PENG[a]
[a]*Institute of Botany, Jiangsu Province and Chinese Academy of Sciences, Nanjing Botanical Garden, Mem. Sun Yat-Sen, Nanjing 210014, China*
[b]*Department of Physics and Materials Science, City University of Hong Kong, Hong Kong*
[c] *Jiangsu Junma Park Technology Co. Ltd, Jiangsu, China*
[d] *Beijing Petrochemical Engineering Corp. LTD, Chaoyang District Tianjuyuan Building No. 7, Beijing, China*

In this work, Ag-AgCl/ZnO hybrid was synthesized via a facial wet chemical method. The synthesized hybrid was characterized by SEM, XRD, EDX, UV-vis spectroscopy and photoluminescence spectroscopy. The Ag-AgCl/ZnO hybrid exhibited a significant enhancement of photocatalytic activity towards degradation of methylene blue under visible light. The cause of the enhanced photocatalytic performance could ascribe to the highly facilitated electron transport by the synergistic effect between ZnO and Ag-AgCl. Meanwhile, Ag-AgCl can implement the photosensitization of ZnO with high efficiency through SPR effect.

(Received November 30, 2014; Accepted January 26, 2015)

Keyword: Hybrid materials; Photocatalyst; ZnO; Ag-AgCl; Visible light

1. Introduction

During the past decade, organic dyes are widely used in many industrial field and their effluents have become of the main components of water pollution. They could easily contaminate the environment as well as threaten human health because their high solubility in water, toxic and stable to against light, temperature, chemical and microbial decompose process [1-4]. Since the photocatalytic activity of TiO_2 has been discovered by Fujishima and Honda in 1972 [5], photocatalysts have been extensively studied for the elimination of organic dyes in wastewater [6-12]. Studies showed that the utilization of commercial semiconductors could mineralize many organic compounds in water, mineral acids and CO_2. Therefore, using the photocatalytic activity of semiconductors to elimination of organic pollutants is deemed to an alternative approach for waste water treatment.

Zinc oxide is a well-known *n*-type semiconductor with band gap energy of 3.37 eV, hence is considered as one of the best photocatalysts to deal with organic pollutant [13, 14]. However, like other metal oxide photocatalysts, the photocatalytic activity of ZnO is still restricted by fast recombination of the photogenerated electron hole pairs [15, 16]. Additionally, the ZnO only can absorb UV light with λ< 387 nm, which means only less than 5% of solar energy can be used for photocatalytic reaction. Many efforts have been made for extending the absorption range of ZnO, such as elements doping and metal-semiconductor heterostructure formation. For example, Ag has been wildly studied for coupling with ZnO and extends the visible light absorption due to the localized surface plasmon resonance (SPR) effect. Also, studies showed the metal particles can act

* Corresponding author: yuhongzhengcas@gmail.com

as a sink for electrons, to prolong the lifetime of the photogenerated charge carriers and therefore improved the photocatalytic activity [17-25].

Silver halides are wildly recognized as photosensitive materials [17, 26-29]. Recently, research showed that the Ag-AgCl supported metal oxide semiconductor has enhanced photocatalytic activity under visible or simulated solar light. For example, Jiaguo Yu *et al.*[30] reported the fabrication and characterization of $Ag/AgCl/TiO_2$ nanotube arrays. The synthesized $Ag/AgCl/TiO_2$ nanotube arrays exhibited a highly visible light photocatalytic activity for photocatalytic degradation of methyl orange in water. Adhikari *et al.*[26] reported the synthesis of $Ag/AgCl/WO_3$ photocatalyst by a microwave assisted hydrothermal method. The Dye degradation efficiency of the composite photocatalyst was found to be increased significantly as compared to that of the commercial WO_3 nanopowder. In this study, we report a facial chemical method for synthesizing Ag-AgCl/ZnO hybrid. The photocatalytic activities of the as-prepared Ag-AgCl/ZnO hybrids are investigated by photodegradation of methylene blue (MB) under the visible light illumination and the performance is compared with the bare ZnO.

2. Experimental

2.1 Materials

Zinc nitrate hexahydrate ($Zn(NO_3)_2{\cdot}6H_2O$), ammonium hydroxide (28-30% NH_3 basis), silver nitrate ($AgNO_3$), methylene blue (MB), benzoquinone (BQ), ammonium oxalate (AO) and isopropanol (IPA) were purchased from Sigma-Aldrich. All other chemicals used were analytical grade reagents without further purification. Milli-Q water (18.2 MΩ cm) was used throughout the experiments.

2.2 Preparation of Ag-AgCl/ZnO hybrid

As-received zinc nitrate hexahydrate (5 g) was dissolved in 20 mL of water under stirring. Then, 1 mL of ammonium hydroxide was added into the solution for 10 min stirring. Afterward, a certain amount of $AgNO_3$ solution (50 mM) was slowly added. After 15 min stirring, 1 mL of NaCl (0.5 M) was slowly added into the formed suspension. Then the suspension was refluxed at 110°C for 30 min. The precipitate was collected by centrifugation followed with water wash. The final product was obtained by calcination of the precipitate in a N2 protected furnace at 200°C for 1 h (denoted as Ag-AgCl/ZnO-1, Ag-AgCl/ZnO-2, Ag-AgCl/ZnO-3 and Ag-AgCl/ZnO-4 for the mole ratios of Zn and Ag set as 3:1, 2:1, 1:1 and 1:2, respectively).

2.3 Characterizations

X-ray diffraction patterns were collected from 20° to 80° in 2θ by a XRD with Cu Kα radiation (D8-Advanced, Bruker, Germany). Surface morphology of samples were analyzed by scanning electron microscope (SEM, S-4700, HITACHI, Japan). The optical absorption was investigated using a UV–vis diffuse reflectance spectrophotometer (U-41000, HITACHI, Tokyo, Japan). Fluorescence emission spectra were collected on a fluorescence spectrophotometer with 315 nm excited source (FP-6500, JASCO, Japan).

2.4 Photocatalytic activity evaluation

Photocatalytic activity of the samples was evaluated by photocatalytic degradation of MB aqueous solution under visible light irradiation. Typically, 50 mg of the prepared sample was added into 20 mL of MB solution (15 mg/L) and kept under dark conditions for 30 min. After light illumination, 2 mL of suspension was then taken out a certain period and the photocatalyst was separated by centrifugation. The absorption of MB was then measured by a UV-vis spectroscopy. The absorbance of MB at 664 nm was used for measuring the concentration change.

3. Results and discussion

SEM was used for observing the morphology of synthesized samples. Figure 1 shows the SEM images of ZnO, Ag-AgCl/ZnO-1, Ag-AgCl/ZnO-2 and Ag-AgCl/ZnO-4. As can be seen, the ZnO formed without Ag-AgCl exhibits a cluster shape, which consists of many small nanorods. In contrast, the ZnO particles formed in the Ag-AgCl/ZnO hybrid show an individual rod structure with length varying from 0.5-1.5 μm. Moreover, the Ag-AgCl particles also observed in the hybrid with a spherical shape. It can be seen that the size of Ag-AgCl particle slightly increases when the mole ratio of Ag increased in the synthesis process. Also, it can be clearly seen that the Ag-AgCl/ZnO-4 shows a much higher content of Ag-AgCl particles than that of Ag-AgCl/ZnO-1.

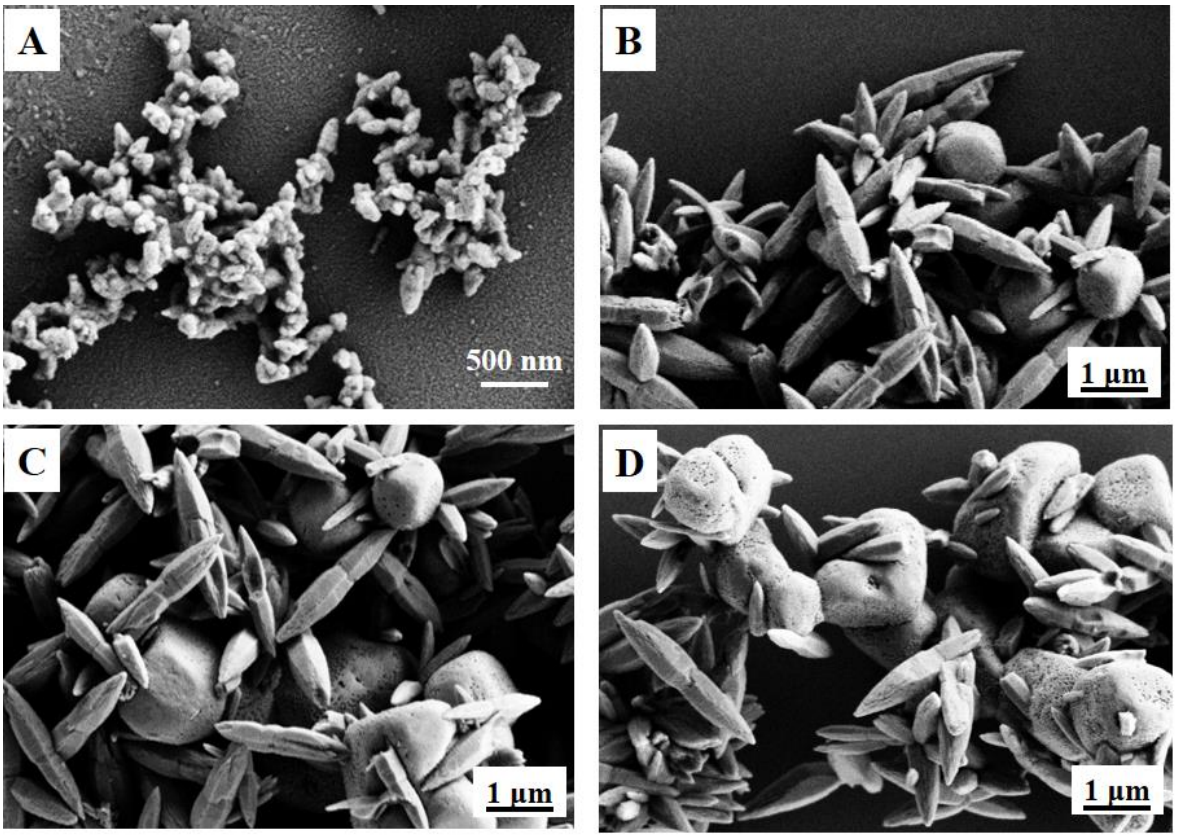

Fig. 1: SEM images of (A) ZnO, (B) Ag-AgCl/ZnO-1, (C) Ag-AgCl/ZnO-2 and (D) Ag-AgCl/ZnO-4.

The elemental information of the as-prepared hybrids was analyzed by EDX. Figure 2A shows the EDX spectrum of Ag-AgCl/ZnO-2. The spectrum presents the only existence of Zn, O, Ag and Cl, indicating the successful formation of hybrid with high purity.

Figure 2B demonstrates the XRD patterns of ZnO, Ag-AgCl/ZnO-1, Ag-AgCl/ZnO-2, Ag-AgCl/ZnO-3 and Ag-AgCl/ZnO-4. The pure ZnO exhibits diffraction peaks at 32.0°, 34.5°, 36.3°, 47.4°, 56.5°, 62.8°, 67.1°, 68.2°, 68.9°, 72.3° and 71.9° can be indexed to hexagonal ZnO (JCPDS 36-1451). In XRD patterns of Ag-AgCl/ZnO samples, the peaks at 26.2°, 45.5°, 54.2°and 56.7° are correspond to the cubic phase crystal structure of AgCl ((JCPDS 31-1238). Moreover, two peaks related to the Ag (JCPDS 04-0783) also been observed at 39.0° and 45.1°. By comparing the patterns of ZnO and Ag-AgCl/ZnO hybrids, the intensity of ZnO diffraction peaks decline along with the amount of $AgNO_3$ increases during the synthesis process, which is agreed with the morphology observed in the SEM images.

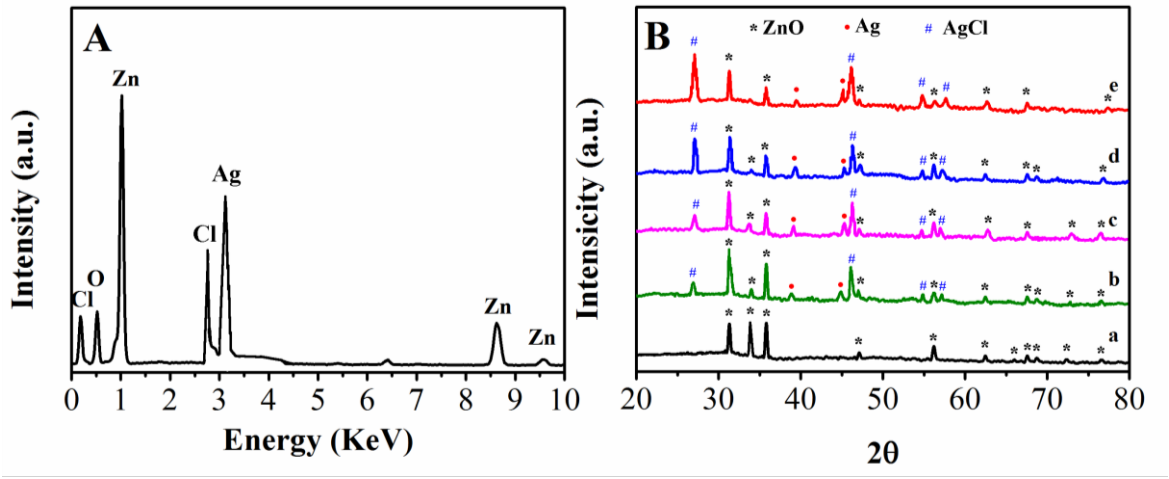

Fig. 2. (A) EDX spectrum of Ag-AgCl/ZnO-2. (B) XRD patterns of (a) ZnO, (b) Ag-AgCl/ZnO-1, (c) Ag-AgCl/ZnO-2, (d) Ag-AgCl/ZnO-3 and (e) Ag-AgCl/ZnO-4.

Fig. 3 displays the UV-vis diffusion reflectance spectra of ZnO, Ag-AgCl/ZnO-1, Ag-AgCl/ZnO-2, Ag-AgCl/ZnO-3 and Ag-AgCl/ZnO-4. It can be seen that the absorption gradually increases with the increases of the Ag-AgCl content. At visible region, the spectrum of ZnO shows no obvious absorption peak. In contrast, the spectra of samples containing Ag-AgCl show obvious SPR characteristic absorption peaks. In Ag-AgCl/ZnO hybrid materials, the intensity of SPR shows a positive relationship with the amount of Ag-AgCl, which is probably due to the increasing amount of Ag particles in the hybrid [31]. Comparing the spectra of Ag-AgCl/ZnO-2 and Ag-AgCl/ZnO-4, it is found that the SPR absorption peak shows a blue-shift. Many studies reported that the SPR absorption of metal can be influenced by its morphology, particle spacing and other around materials [32-34]. In our case, the blue-shift probably caused by the increasing of the small number of Ag nanoparticles provide by the high concentration of $AgNO_3$ [35].

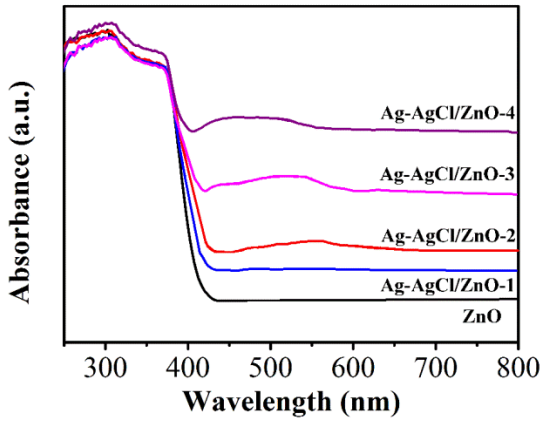

Fig 3: UV-vis spectra of ZnO, Ag-AgCl/ZnO-1, Ag-AgCl/ZnO-2, Ag-AgCl/ZnO-3 and Ag-AgCl/ZnO-4.

The photocatalytic activities of prepared photocatalysts were investigated by photodegradation of MB, a common azo dye used in the textile industry, under visible light irradiation. As shown in Figure 4A, the MB itself cannot be degraded after 120 min light irradiation when the absence of any photocatalyst. However, the MB can be degraded when the presence of pure ZnO. After 120 min light irradiation, about 50% of MB molecules have been degraded in the solution. Furthermore, the Ag-AgCl/ZnO hybrids exhibited much higher degradation efficiencies than pure ZnO. It can be seen that the photocatalytic performance of the hybrid increased from the Ag-AgCl/ZnO-1 to Ag-AgCl/ZnO-2, then decreased with the persistent

increase of Ag-AgCl content. Therefore, in our case, the best mole ratio of Zn and Ag is 2:1. The apparent constant values of each photocatalyst can be calculated from the linear fitting of $\ln(C_0/C_t)$ vs irradiation time. As shown in Figure 4B, the apparent constant values of ZnO, Ag-AgCl/ZnO-1, Ag-AgCl/ZnO-2, Ag-AgCl/ZnO-3 and Ag-AgCl/ZnO-4 are 0.00531, 0.00852, 0.03995, 0.01874 and 0.00568/min, respectively, indicating that the Ag-AgCl/ZnO-2 hybrid has remarkably enhanced photocatalytic activity.

The TOC content also been monitored during the photodegradation process. Figure 4C displays the kinetic linear simulation curves based on the Langmuir–Hinshelwood first-order kinetic model. The results show that the TOC content decreased with photodegradation time, indicating the degradation of MB into nontoxic compounds.

It is generally known that the calcination temperature can influence the size and crystallization of photocatalysts [36]. In order to evaluate the influence of calcination temperature on the photocatalytic performance, the Ag-AgCl/ZnO-2 was calcined at 250, 300, 350, 400 and 450°C and the results were depicted in Figure 4D. The degradation profiles show that the Ag-AgCl/ZnO-2 calcined at 200°C has the best photocatalytic performance. Ascribe to the aggregation and crystalline growth of Ag-AgCl/ZnO in the high temperature, increasing of calcination temperature of Ag-AgCl/ZnO-2 gives the lower photocatalytic activity [37].

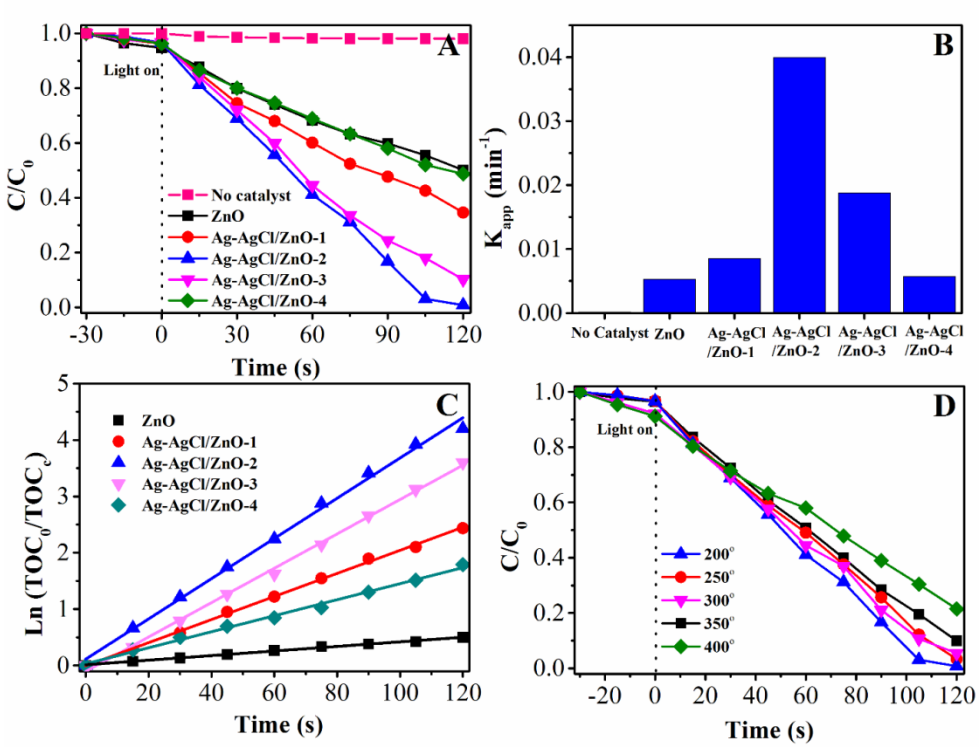

Fig. 4: (A) The photocatalytic degradation of MB by different photocatalysts. (B) The apparent reaction rate constant of different photocatalysts. (C) The ln(TOCo/TOC$_t$) vs time curves of mineralization of MB by different photocatalysts. (D) The photocatalytic degradation of MB using Ag-AgCl/ZnO-2 calcined at different temperatures.

It is well known that heterogeneous photocatalytic system can produce reactive species after irradiation of photocatalyst [38-40]. In order to study the reactive species during photodegradation of MB under visible light irradiation, terephthalic acid photoluminescence probing technique was first employed for detecting the formation of •OH [41]. Figure 5A shows the room temperature PL emission spectra of terephthalic acid solution collected every 15 min of irradiation. It can be seen that the PL intensity showed a constant emission after the irradiation, indicating only small amount of •OH radicals are formed during the photodegradation process. This confirms that the •OH radicals are not the main active species in the degradation process. In

addition, the effects of various scavengers (1 mM) on photodegradation were studied and the corresponding results are shown in Figure 5B. Without using any scavenger, the degradation of MB on the Ag-AgCl/ZnO-2 was found to be 99%. However, the photodegradation efficiency declined dramatically to about 20% with addition of AO (a scavenger of h^+) [42]. Moreover, the addition of BQ (a scavenger of $\bullet O_2^-$) [43] and IPA (a scavenger of •OH) [42] also showed a slight decrease of photodegradation efficiency. Therefore, considering the results of both experiments, it can be concluded that holes are the dominating active species for the photodegradation of MB on the Ag-AgCl/ZnO hybrid.

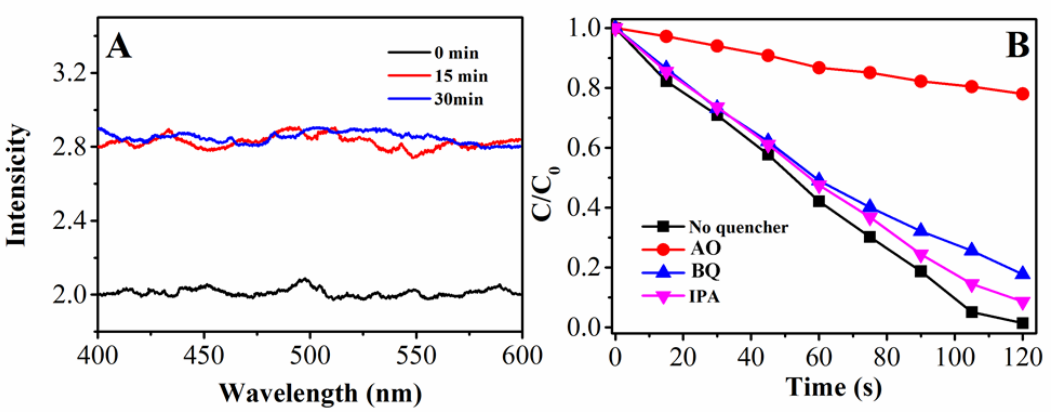

Fig. 5: (A) •OH trapping PL spectral changes collected during the visible illumination of Ag-AgCl/ZnO-2 in a 0.5 mM terephthalic acid solution. (B) Photodegradation of MB using Ag-AgCl/ZnO-2 as photocatalyst when the presence of different quenchers.

The stability of photocatalyst during photocatalytic reaction is an important factor in the practical applications. Therefore, the reusability test of the synthesized photocatalyst was also conducted using Ag-AgCl/ZnO-2 for eight photodegradation cycles. As shown in Figure 6, the Ag-AgCl/ZnO-2 still remains more than 70% of photocatalytic activity after eight cycles photodegradation, indicating that the hybrid was quite stable for reproducibility.

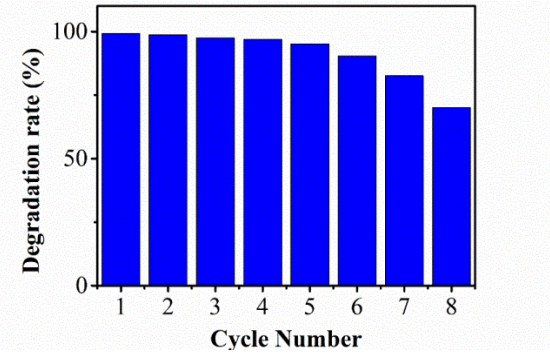

Fig. 6: Recycle tests of the Ag-AgCl/ZnO-2.

In general, the heterojunction interfaces will be constructed between the components of hybrid materials, which could facilitate the transfer of the photogenerated carriers and enhance the photocatalytic performance of semiconductor. [44] In this case, the Fermi levels of ZnO, AgCl, and Ag could be balanced to the same position, leading to the electron transfer and exchange. The surface plasmon could form on the Ag surface when the frequency of the incident light matches the electron oscillation. Then, the electrons in Ag Fermi level are excited and transformed into excited electrons. These excited electrons could transfer to the conduction band of AgCl and ZnO for achieving the sensitizing effect of ZnO. These electrons further transfer to O_2 to create active oxidants. Therefore, this electron transfer process should facilitate the photoexcited electron to be

separated from recombination with the hole. In order to confirm the suppression of electron hole pair recombination, the PL emission spectra of ZnO and Ag-AgCl/ZnO-2 was collected for comparison. As shown in Figure 7, the PL spectrum of ZnO present a wide emission band in the wavenumber range from 330 to 550 nm. The UV peaks (~350-380 nm) are assigned to the recombination of the photogenerated electron hole pairs.[45] The visible emission band (~520-570 nm) is assigned to the recombination of electrons caused by structural defects such as zinc vacancies, oxygen vacancies and interstitial oxygen.[46] In contrast, the PL spectrum of Ag-AgCl/ZnO-2 shows a significant decline of the emission intensity, implying that the rate of electron hole pair recombination has been suppressed.

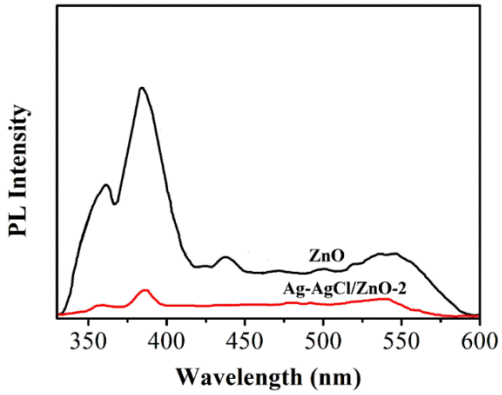

Fig. 7: PL spectra of ZnO and Ag-AgCl/ZnO-2.

4. Conclusion

In conclusion, we have demonstrated that Ag-AgCl/ZnO hybrid can be prepared via a facial wet chemical method using $Zn(NO_3)_2 \cdot 6H_2O$ and AgNO3 as raw materials. In this way, ZnO nanorods and Ag-AgCl micro-spheres were obtained synchronously. The results of photodegradation experiments showed that the Ag-AgCl/ZnO hybrid has a much higher photocatalytic activity than pure ZnO. The best photocatalytic performance was achieved when the mole ratios of Zn and Ag was 2:1. The enhanced photocatalytic activity is due to introduction of Ag-AgCl, which increases the electrons and holes separation efficiency and transfer speed. Meanwhile, ZnO is able to respond to visible light through the SPR effect produced by the Ag-AgCl.

Reference

[1] T.M. Fonovich, Drug Chem Toxicol **36,** 343 (2013).
[2] S.A. Haughey, P. Galvin-King, Y.-C. Ho, S.E.J. Bell, C.T. Elliott, Food Control **In press,** (2014).
[3] A. Hakeem, A. Shakoor, M. Irfan, Ali.I., M. Azhar Khan, B.M. Naeem Ashiq, M. Ishaq, A. A., Journal of Ovonic Research **10,** 149 (2014).
[4] I. M.A., K.S. Rahman, F. Haque, N. Dhar, M. Salim, M. Akhtaruzzaman, K. Sopian, N. Amin, Journal of Ovonic Research **10,** 185 (2014).
[5] A. Fujishima, K. Honda, Nature **238,** 37 (1972).
[6] W.F. Khalik, S.-A. Ong, L.-N. Ho, Y.-S. Wong, N.A. Yusoff, F. Ridwan, Desalination and Water Treatment 1 (2014).
[7] Alka, K.M. Choi, Y.H. Kim, S.M. Lee, Desalination and Water Treatment **51,** 3076 (2013).
[8] E.S. Sazali, R. Sahar, S.K. Ghoshal, S. Rohani, R. Arifin, Journal of Non-Oxide Glasses **6,** 61 (2014).
[9] S. Suresh, Journal of Non-Oxide Glasses **6,** 47 (2014).
[10] D. Thomas, S. Augusine, J. Parakash, Journal of Optoelectronic and Biomedical Materials

6, 101 (2014).
[11] A. Ayeshamariam, M. Kashif, V.S. Vidhya, M.G. Sankaracharyulu, V. Swaminathan, M. Bououdina, M. Jayachandran, Journal of Optoelectronic and Biomedical Materials **6,** 85 (2014).
[12] A. Wang, H.P. Ng, Y. Xu, Y. Li, Y. Zheng, J. Yu, F. Han, F. Peng, L. Fu, Journal of Nanomaterials **2014,** 6 (2014).
[13] A. Khani, M.R. Sohrabi, M. Khosravi, M. Davallo, Turkish J. Eng. Env. Sci. **37,** 91 (2013).
[14] C. Zhang, J. Zhang, Y. Su, M. Xu, Z. Yang, Y. Zhang, Physica E **56,** 251 (2014).
[15] Q. Wang, N. Plylahan, M.V. Shelke, R.R. Devarapalli, M. Li, P. Subramanian, T. Djenizian, R. Boukherroub, S. Szunerits, Carbon **68,** 175 (2014).
[16] A. Wei, L. Xiong, L. Sun, Y. Liu, W. Li, W. Lai, X. Liu, L. Wang, W. Huang, X. Dong, Mater Res Bull **48,** 2855 (2013).
[17] B. Xue, T. Sun, J.K. Wu, F. Mao, W. Yang, Ultrason Sonochem **22,** 1 (2015).
[18] J. Low, J. Yu, Q. Li, B. Cheng, Phys Chem Chem Phys **16,** 1111 (2014).
[19] C. Sima, L. Ion, C. Grigoriu, T.L. Mitran, S. Antonhe, Digest Journal of Nanomaterials and Biostructures **9,** 1479 (2014).
[20] C.P. Ganea, L. Frunza, I. Zgura, N. Preda, E. Matel, S. Frunza, Digest Journal of Nanomaterials and Biostructures **9,** 1493 (2014).
[21] N. Preda, M. Enculescu, A. Florica, A. costas, A. eEvanghelidis, E. Matei, I. Enculescu, Digest Journal of Nanomaterials and Biostructures **8,** 1590 (2014).
[22] S. Vishnoi, R. Kumar, B.P. Singh, Journal of Intense Pulsed Lasers and Applications in Advanced Physics **4,** 35 (2014).
[23] R. Manoj, M.K. Jayaraj, Journal of Intense Pulsed Lasers and Applications in Advanced Physics **2,** 11 (2014).
[24] P. Muthukumar, C. Rangasami, S. Ganesan, Chalcogenide Letters **10,** 113 (2013).
[25] R. Jeyachitra, P. Rajasekaran, V. Senthilnathan, Chalcogenide Letters **11,** 303 (2014).
[26] R. Adhikari, G. Gyawali, T. Sekino, S. Wohn Lee, J Solid State Chem **197,** 560 (2013).
[27] L. Fu, A. Wang, Y. Zheng, W. Cai, Z. Fu, Materials Letters **142,** 119 (2015).
[28] L. Fu, Z. Fu, Ceram Int **41,** 2492 (2015).
[29] L. Fu, W. Cai, A. Wang, Y. Zheng, Materials Letters **142,** 201 (2015).
[30] J. Yu, G. Dai, B. Huang, J Phys Chem C **113,** 16394 (2009).
[31] W. Li, F. Hua, J. Yue, J. Li, Appl Surf Sci **285,** 490 (2013).
[32] S. Linic, P. Christopher, D.B. Ingram, Nat Mater **10,** 911 (2011).
[33] K.L. Kelly, E. Coronado, L.L. Zhao, G.C. Schatz, J Phys Chem B **107,** 668 (2002).
[34] A. Moores, F. Goettmann, New J Chem **30,** 1121 (2006).
[35] Y. Tang, Z. Jiang, G. Xing, A. Li, P.D. Kanhere, Y. Zhang, T.C. Sum, S. Li, X. Chen, Z. Dong, Z. Chen, Adv Funct Mater **23,** 2932 (2013).
[36] S.-Y. Kim, T.-H. Lim, T.-S. Chang, C.-H. Shin, Catal Lett **117,** 112 (2007).
[37] M. Pirhashemi, A. Habibi-Yangjeh, J Alloy Compd **601,** 1 (2014).
[38] E. Grabowska, J. Reszczyńska, A. Zaleska, Water Res **46,** 5453 (2012).
[39] K. Nakata, A. Fujishima, J Photoch Photobio C **13,** 169 (2012).
[40] M. Pelaez, N.T. Nolan, S.C. Pillai, M.K. Seery, P. Falaras, A.G. Kontos, P.S.M. Dunlop, J.W.J. Hamilton, J.A. Byrne, K. O'Shea, M.H. Entezari, D.D. Dionysiou, Appl Ctatl B-Environ **125,** 331 (2012).
[41] Q. Xiao, Z. Si, J. Zhang, C. Xiao, X. Tan, J. Hazard. Mater. **150,** 62 (2008).
[42] G. Li, K.H. Wong, X. Zhang, C. Hu, J.C. Yu, R.C.Y. Chan, P.K. Wong, Chemosphere **76,** 1185 (2009).
[43] N. Zhang, S. Liu, X. Fu, Y.-J. Xu, J Phys Chem C **115,** 9136 (2011).
[44] C. Liu, H. Lin, S. Gao, P. Yin, L. Guo, B. Huang, Y. Dai, B Kor Chem Soc **35,** 441 (2014).
[45] H. Raj Pant, B. Pant, H. Joo Kim, A. Amarjargal, C. Hee Park, L.D. Tijing, E. Kyo Kim, C. Sang Kim, Ceram Int **39,** 5083 (2013).
[46] J.H. Yang, J.H. Zheng, H.J. Zhai, L.L. Yang, Cryst Res Technol **44,** 87 (2009).